



**The Effect of Tempering and Aging on a Low  
Activation Martensitic Steel**

**R.D. Griffin, R.A. Dodd, G.L. Kulcinski, D.S. Gelles**

**January 1989**

**UWFDM-784**

***FUSION TECHNOLOGY INSTITUTE***

***UNIVERSITY OF WISCONSIN***

***MADISON WISCONSIN***

### **DISCLAIMER**

This report was prepared as an account of work sponsored by an agency of the United States Government. Neither the United States Government, nor any agency thereof, nor any of their employees, makes any warranty, express or implied, or assumes any legal liability or responsibility for the accuracy, completeness, or usefulness of any information, apparatus, product, or process disclosed, or represents that its use would not infringe privately owned rights. Reference herein to any specific commercial product, process, or service by trade name, trademark, manufacturer, or otherwise, does not necessarily constitute or imply its endorsement, recommendation, or favoring by the United States Government or any agency thereof. The views and opinions of authors expressed herein do not necessarily state or reflect those of the United States Government or any agency thereof.

**The Effect of Tempering and Aging on a Low  
Activation Martensitic Steel**

R.D. Griffin, R.A. Dodd, G.L. Kulcinski, D.S.  
Gelles

Fusion Technology Institute  
University of Wisconsin  
1500 Engineering Drive  
Madison, WI 53706

<http://fti.neep.wisc.edu>

January 1989

UWFDM-784

THE EFFECT OF TEMPERING AND AGING ON A  
LOW ACTIVATION MARTENSITIC STEEL

R.D. Griffin, R.A. Dodd, G.L. Kulcinski  
Fusion Technology Institute  
Department of Nuclear Engineering and Engineering Physics  
University of Wisconsin

1500 Johnson Drive  
Madison, WI 53706

and

CONFIDENTIAL  
UNCLASSIFIED  
DATE 01/14/00 BY 60322 UCBAW/BJS

D.S. Gelles  
Battelle Pacific Northwest Laboratory  
P.O. Box 999  
Richland, WA 99352

January 1989

## ABSTRACT

A recent requirement for candidate materials for fusion reactors is that the induced radioactivity decay to relatively low levels within one hundred to five hundred years. A martensitic steel has been designed to meet this requirement. The composition of the steel in weight percent is 11.81% Cr, 0.097% C, 0.28% V, 0.89% W, 6.4% Mn, and 0.11% Si. Tempering and aging studies have been done to characterize the material. The tempering conditions studied were two hours at 400, 500, 600, 700, 800, and 900 C, and 24 hours at 500 and 700°C. Aging conditions were 1000 and 5000 hours at 365, 420, 520, and 600°C. Microhardness, optical metallography, and electron microscopy were used to examine the samples. The microhardness and electron microscopy results indicated that the  $A_{c1}$  in this steel lies between 700 and 800°C. The primary precipitate which formed was  $M_{23}C_6$ . A manganese rich chi phase was also seen in the samples aged at 420 and 520°C.

## INTRODUCTION

Ferritic and martensitic steels are being considered as candidate materials for the first wall of fusion reactors because of their swelling resistance and their mechanical properties. A more recent requirement for these steels is for their radioactivity to decay to relatively low levels within one hundred to five hundred years. To reach this goal, alloying changes in the current steels must be made. The steel of this study, L9, was provided by Battelle Pacific Northwest Laboratories. The steel is a 12% chromium alloy which is designed to be fully martensitic when air cooled. The composition of L9 and HT-9 is shown in Table 1. HT-9 is another 12% chromium martensitic steel which has been considered for fusion reactor use, although it is not a low-activation alloy. Compared with HT-9, the carbon content of L9 was reduced and to achieve the desired decay in activation the nickel and molybdenum were eliminated. The tungsten content of L9 was increased to replace the molybdenum, in order to preserve high temperature strength. The tungsten level was held at 1% to avoid intermetallic formation. Nickel and carbon are austenite stabilizers, and their loss was compensated for by increasing the manganese content. Although neutron irradiation results on L9 have been published,<sup>(1-5)</sup> there has not been a study of the response of this steel to heat treatment. In this work, this omission is addressed.

## EXPERIMENTAL PROCEDURE

The alloy was received in the rolled condition and was first normalized at 1000°C for twenty hours followed by an air cool to room temperature, and then reheated to 1100°C for ten minutes and allowed again to air cool to room temperature. To determine the tempering response of the steel it was held for

Table 1. The Composition of HT-9 and L9 in Weight Percent

	<u>HT-9</u>	<u>L9</u>
Cr	12	11.81
C	0.20	0.097
V	0.3	0.28
W	0.5	0.89
Mn	0.6	6.47
Ni	0.5	---
Mo	1.0	---
S	≤ 0.072	0.005
Si	0.4	0.11
N	---	0.003
P	≤ 0.03	≤ 0.005

two hours at 400, 500, 600, 700, 800 and 900°C, and for twenty-four hours at 500 and 700°C. Steels which were aged first received a two hour temper at 700°C, and then were aged for one thousand and five thousand hours at 365, 420, 520, and 600°C. Optical metallography, microhardness and transmission electron microscopy (TEM) were used to characterize the heat treated steel.

## RESULTS

The steel formed a fully martensitic structure when air cooled as shown in the optical images of the rolled, normalized, and normalized and tempered steel (Fig. 1). In many of the images, prior austenite grain boundaries are visible. The average size of these grains was 120  $\mu\text{m}$ .

Figure 2 shows the Vickers microhardness results for the austenitized and tempered steel. The hardness dropped sharply when the steel was tempered between 500 and 700°C and then increased for tempering temperatures greater than 700°C. This increase indicated austenite formation with subsequent martensite transformation on cooling to room temperature.

In Fig. 3, TEM images of the precipitates extracted from the tempered steel are shown. The precipitates which formed during the 400 and 500°C, two hour temper were within the martensite laths as elongated multigrains, and were tentatively identified as  $\text{M}_3\text{C}$  (Figs. 3a and 3b). Figure 4 shows an energy dispersive X-ray (EDS) spectrum from one of these precipitates. The metal composition of this phase in weight percent was approximately 65% Fe, 30% Cr and 5% Mn. The precipitates in the sample tempered for twenty-four hours at 500°C were a mixture of  $\text{M}_3\text{C}$  and  $\text{M}_{23}\text{C}_6$  (Fig. 3c). The  $\text{M}_{23}\text{C}_6$  tended to be somewhat rounder and single grain, although their shape varied. At 600°C and higher,  $\text{M}_{23}\text{C}_6$  was the only precipitate which was found (Figs. 3d to 3h).

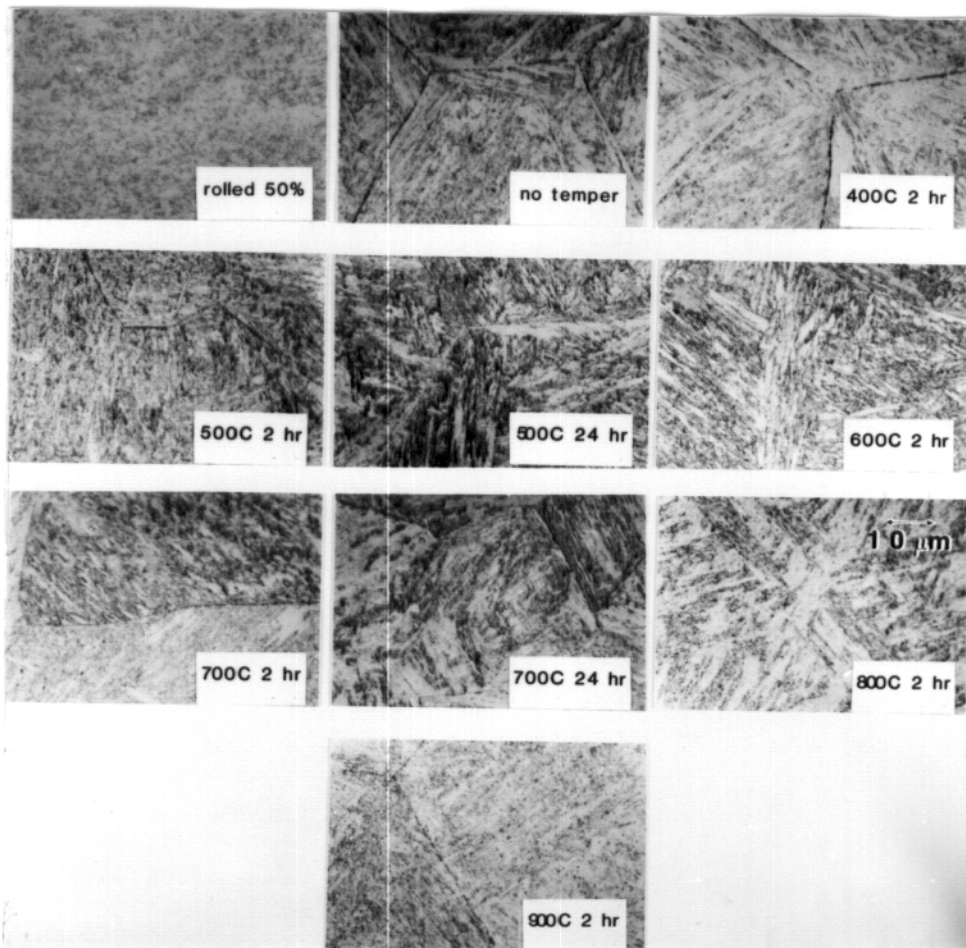


Figure 1. Optical images of L9 in the rolled, normalized, and the normalized and tempered conditions.

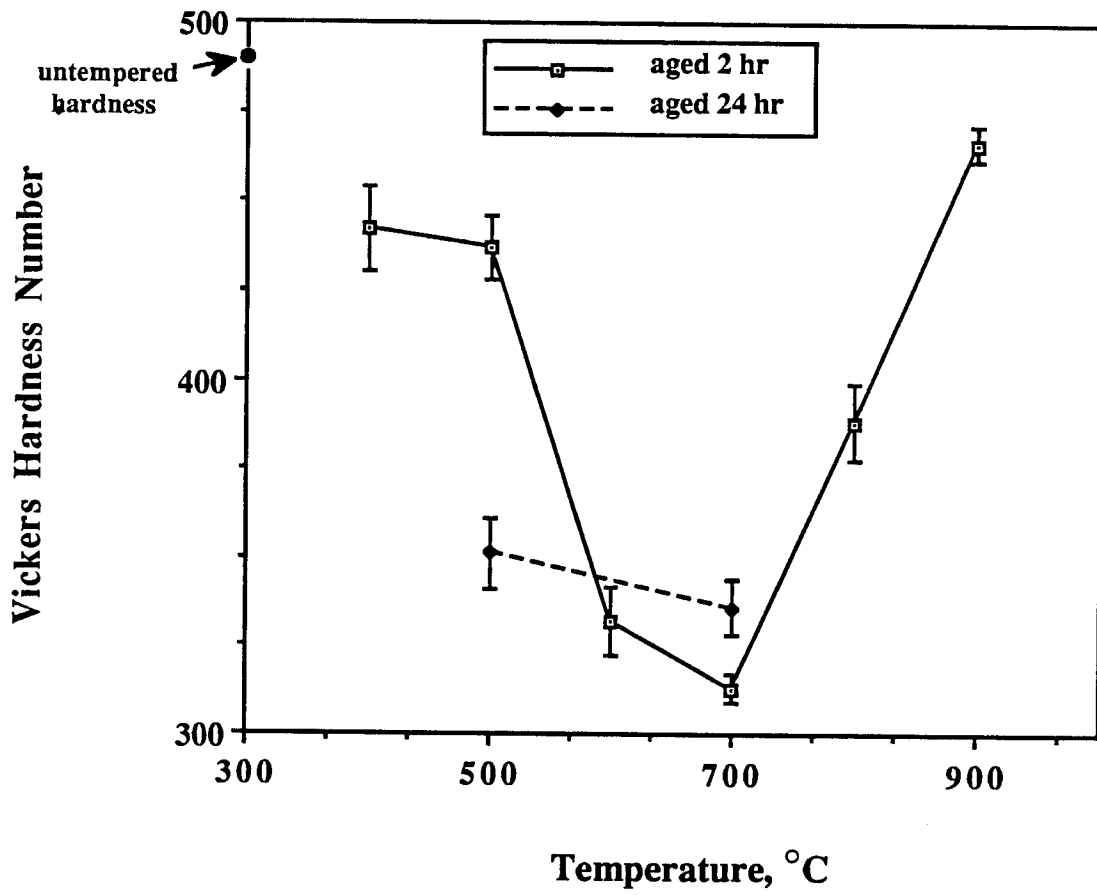


Figure 2. Vickers microhardness results from L9 in the normalized only and the normalized and tempered conditions.

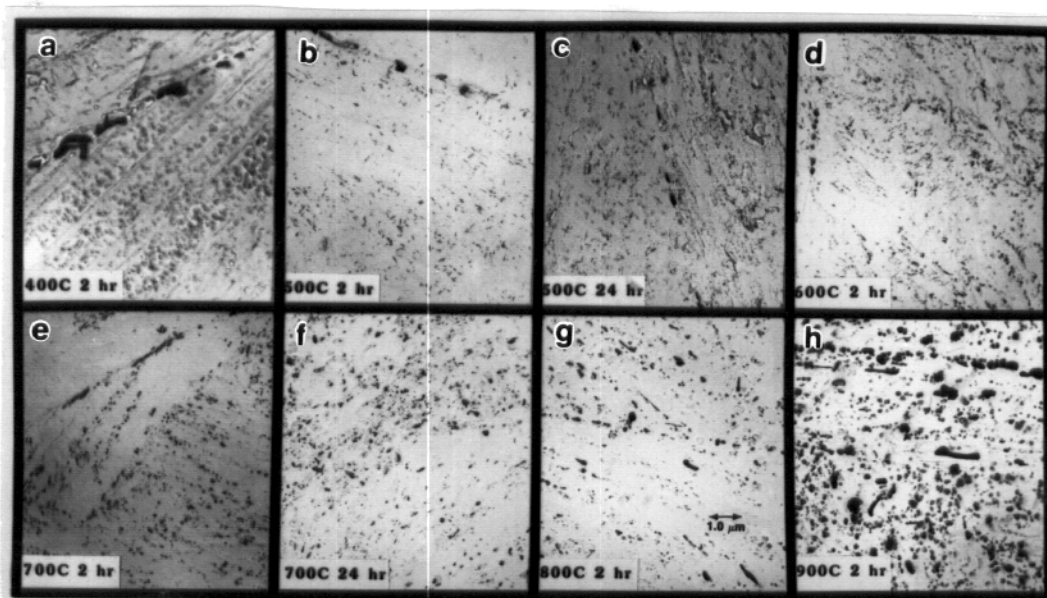


Figure 3. TEM images of extracted precipitates from normalized and tempered L9.

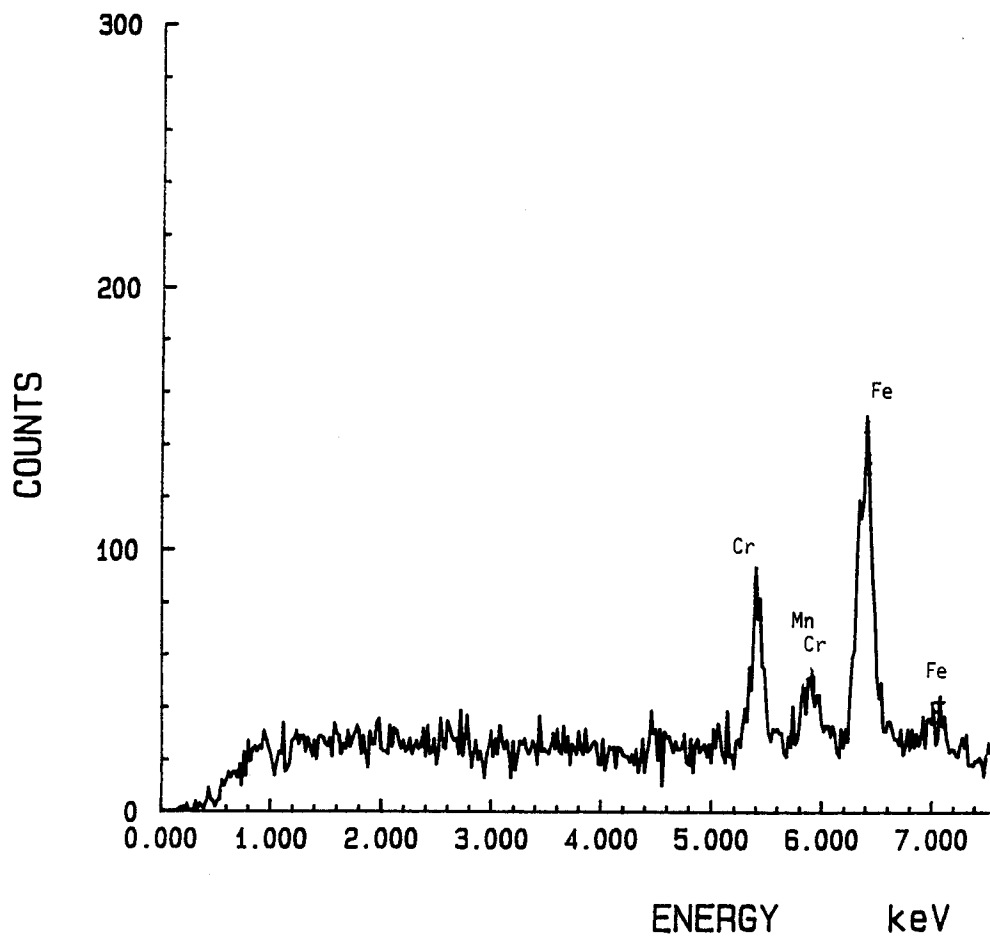


Figure 4. EDS spectrum from the phase which has been tentatively identified as  $M_3C$ .

The two hour tempers at 600°C and 700°C caused the  $M_{23}C_6$  to form mostly at lath boundaries (Fig. 3d and 3e), while tempering at 700°C for 24 hours and 800 and 900°C for two hours led to formation both at the lath boundaries and within the laths (Figs. 3f to 3h). Most of the images in Fig. 3 contain prior austenite grain boundaries which were dotted with precipitates. At all the tempering temperatures the grain boundary precipitates were identified as  $M_{23}C_6$ . The analysis from  $M_{23}C_6$  is shown in Fig. 5. An EDS spectrum from  $M_{23}C_6$  is shown in Fig. 5a. The metal composition of  $M_{23}C_6$  was approximately 58% Cr, 27% Fe, 10% W, 3% Mn and 2% V. Two micro-diffraction patterns used to identify the phase are shown in Figs. 5b and 5c.

In the course of examination, two types of inclusions were found scattered throughout the samples. Figures 6 and 7 represent the results of the analysis on these inclusions. Figures 6a and 6b are TEM images of MnS. Figure 6c is a MnS EDS spectrum and Figs. 6d and 6e are its electron micro-diffraction patterns. The MnS particles were large round particles which were generally seen in groups. Figure 7a is an image of the second type of inclusion found, which has been identified as a spinel, an oxide seen in the steel when it was tempered at temperatures above 500°C. This image shows the typical rectangular shape of the phase. Figure 7b shows its EDS spectrum, rich in manganese and chromium. The small amounts of titanium and aluminum in the oxide must have originated during the steel's fabrication and are probably not uniformly distributed as they were not seen in the vendor's compositional analysis. Figure 7c, 7d and 7e are two characteristic convergent beam electron diffraction patterns from spinel.

The TEM thin foil images of the tempered and untempered steel are shown in Fig. 8. The untempered steel consisted of lath martensite with a very high

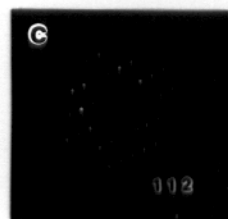
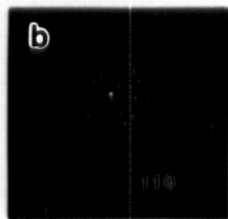
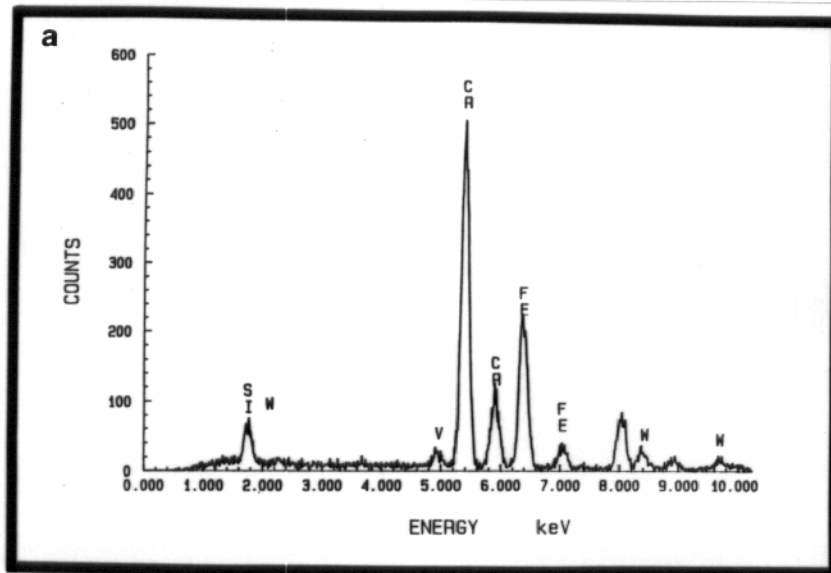


Figure 5. Results from the TEM analysis of  $M_{23}C_6$ . a) A typical EDS spectrum from  $M_{23}C_6$ ; b and c) Micro-diffraction patterns from  $M_{23}C_6$ .

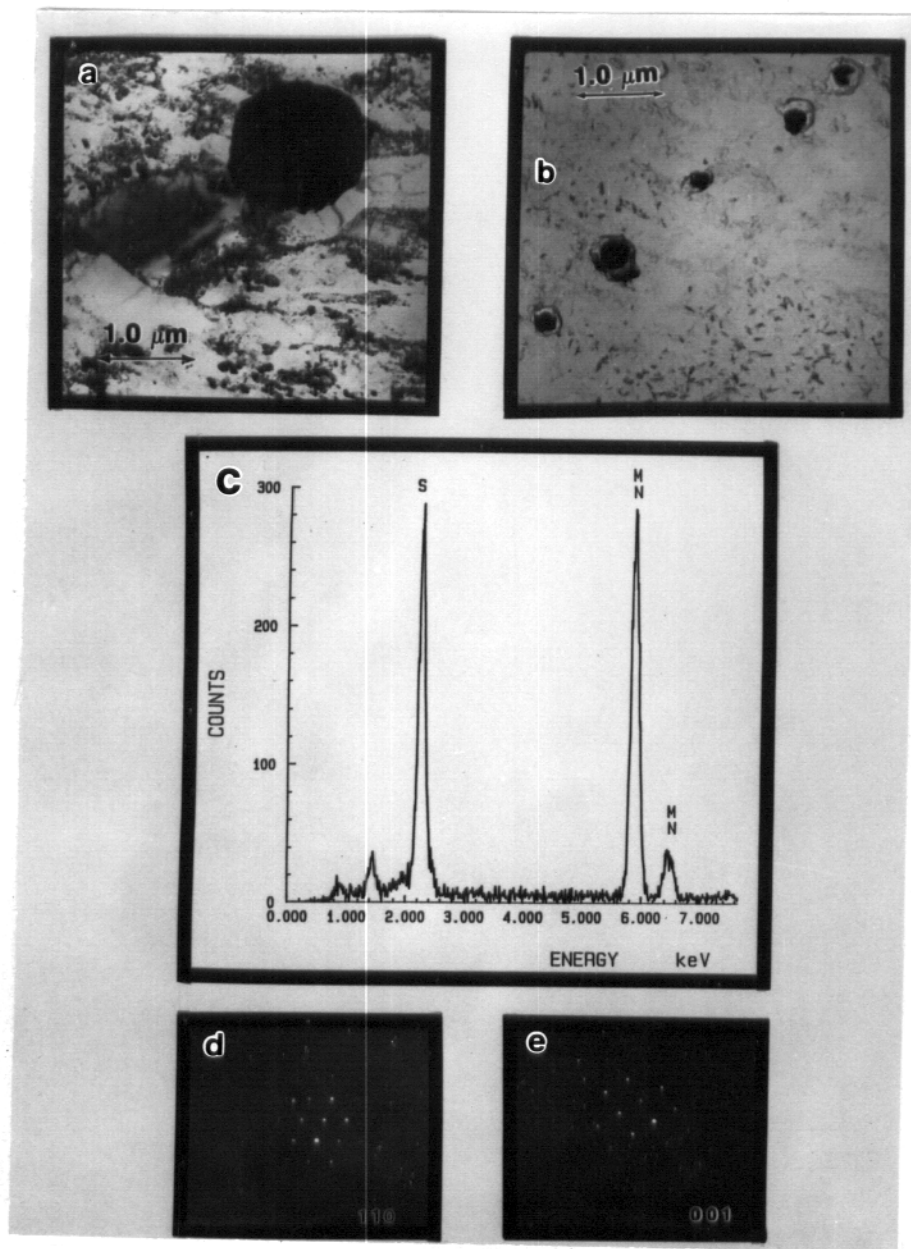


Figure 6. a and b) TEM images of MnS; c) EDS spectrum from MnS; d and e) micro-diffraction patterns from MnS.

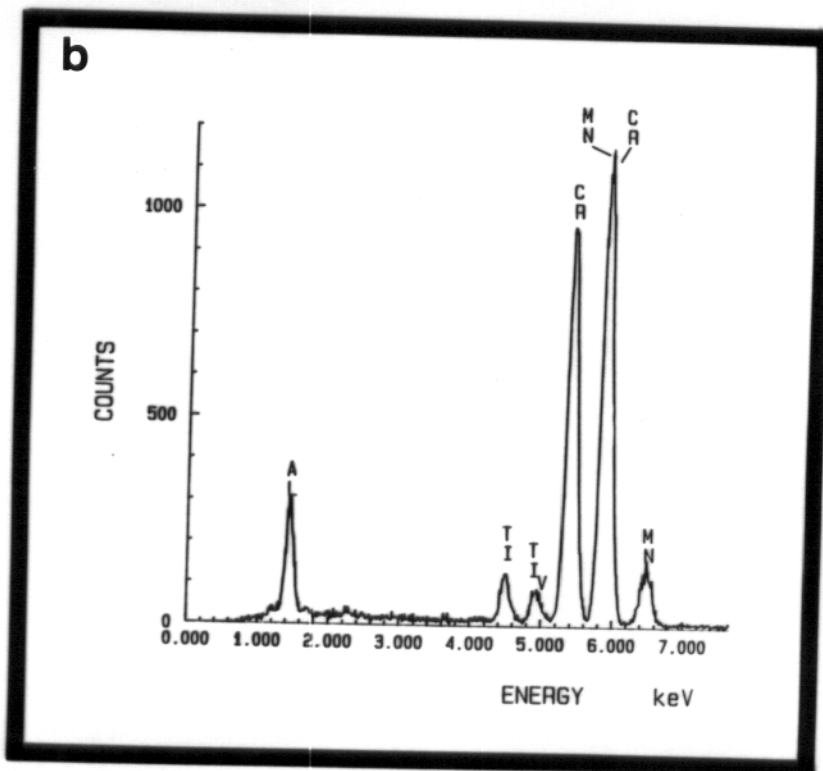


Figure 7. a) TEM image of spinel; b) A typical EDS spectrum from spinel.

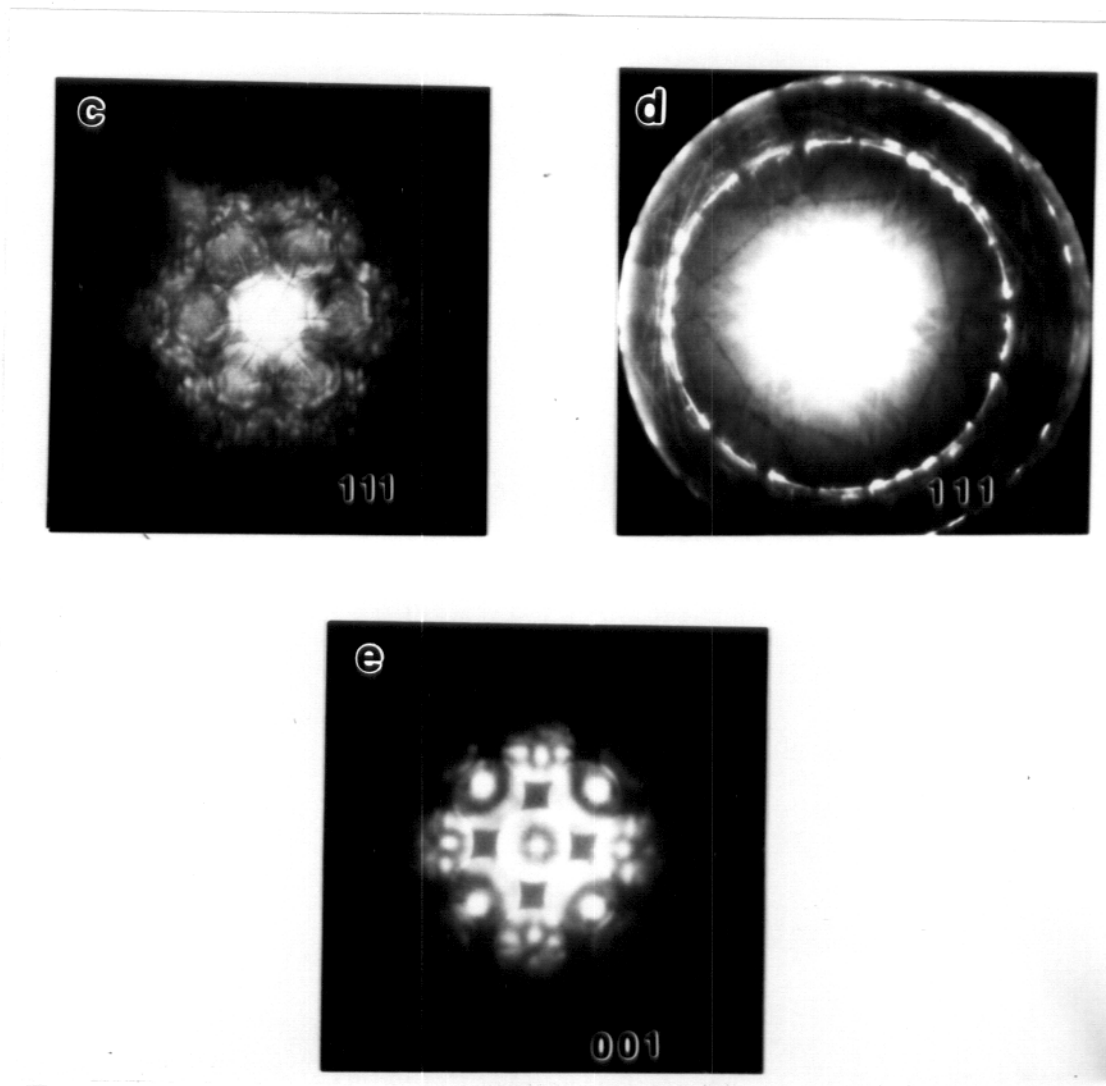


Figure 7. c, d and e) Characteristic convergent beam diffraction patterns from spinel.

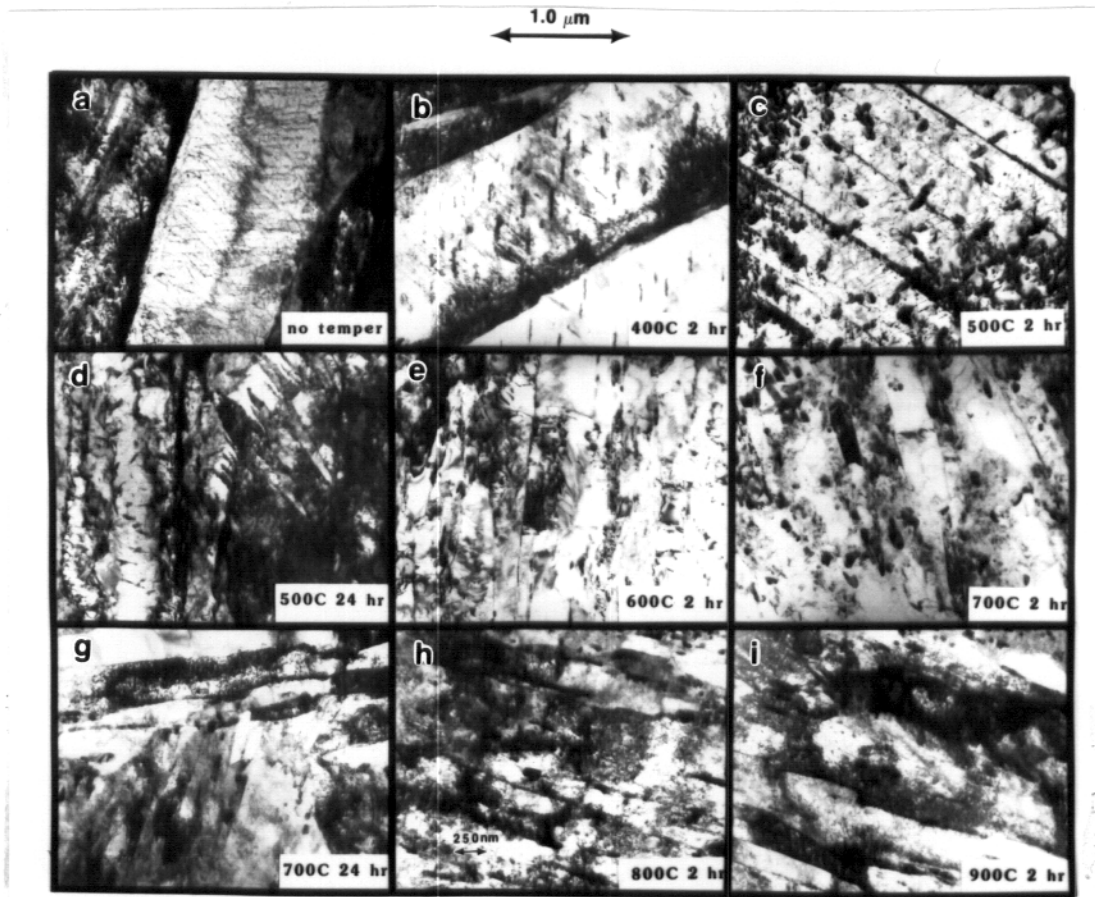


Figure 8. TEM images of the normalized only and the normalized and tempered L9.

dislocation density which was distributed throughout the laths (Fig. 8a). No precipitates were present. Tempering between 400°C and 700°C caused the dislocation structure to begin to recover and rearrange itself so that some areas within the laths were relatively dislocation free (Fig. 8b to 8g). At 800°C and 900°C, the dislocation density became higher and more uniform in some areas, indicating the new untempered martensite had formed (Fig. 8h and 8i).

In Fig. 9, a set of optical micrographs of the tempered steel aged for 1000 and 5000 hours is shown. The samples aged at the lower temperatures looked similar to the tempered steel while at the higher temperatures the martensite laths appear less jagged and more uniform. The Vickers microhardness results for the 1000 and 5000 hour aging treatments are shown in Fig. 10. Again at the two lower temperatures, the results were similar to the steel tempered at 700°C, but at the higher temperatures the hardness is somewhat less. Figure 11 and 12 contain sets of TEM images from the samples aged at temperatures in the range of 365 to 600°C for 1000 and 5000 hours respectively. The aged samples appeared to be similar to the tempered material. However, the samples aged at 520 and 600°C show a somewhat lower dislocation density and the lath boundaries often showed sets of regular dislocations lined up along them. The precipitate structure was also much coarser. These differences were most easily seen for the steels aged for 5000 hours. Another interesting feature seen in the samples aged at these temperatures was the occasional appearance of equiaxed grains which were free of dislocations and contained few, if any precipitates in them. Figure 13 shows one of these grains in the steel aged at 520°C for 5000 hours. These grains were ferrite grains which probably recrystallized during the aging.

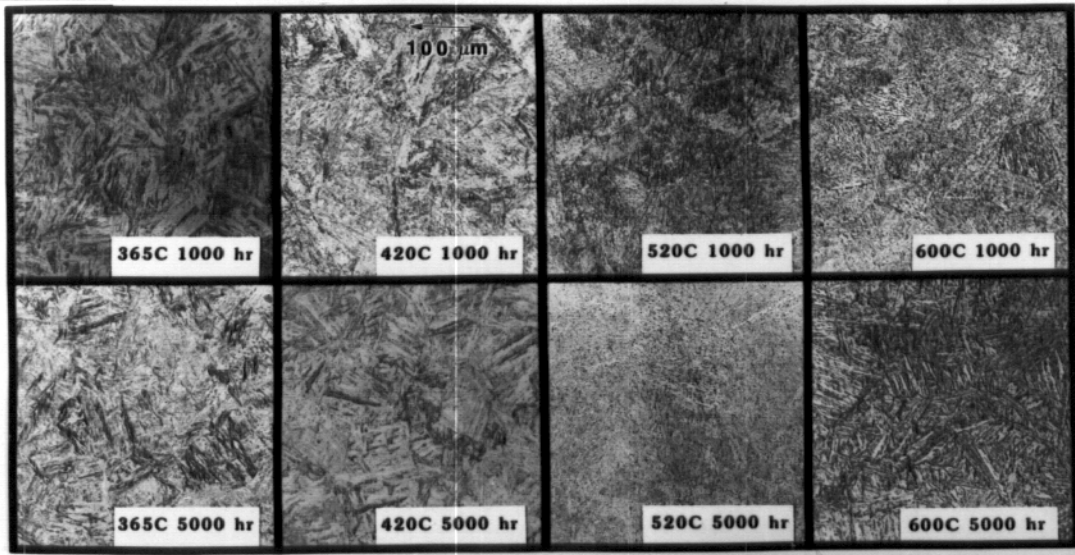


Figure 9. Optical metallographs from L9 aged for 1000 and 5000 hours.

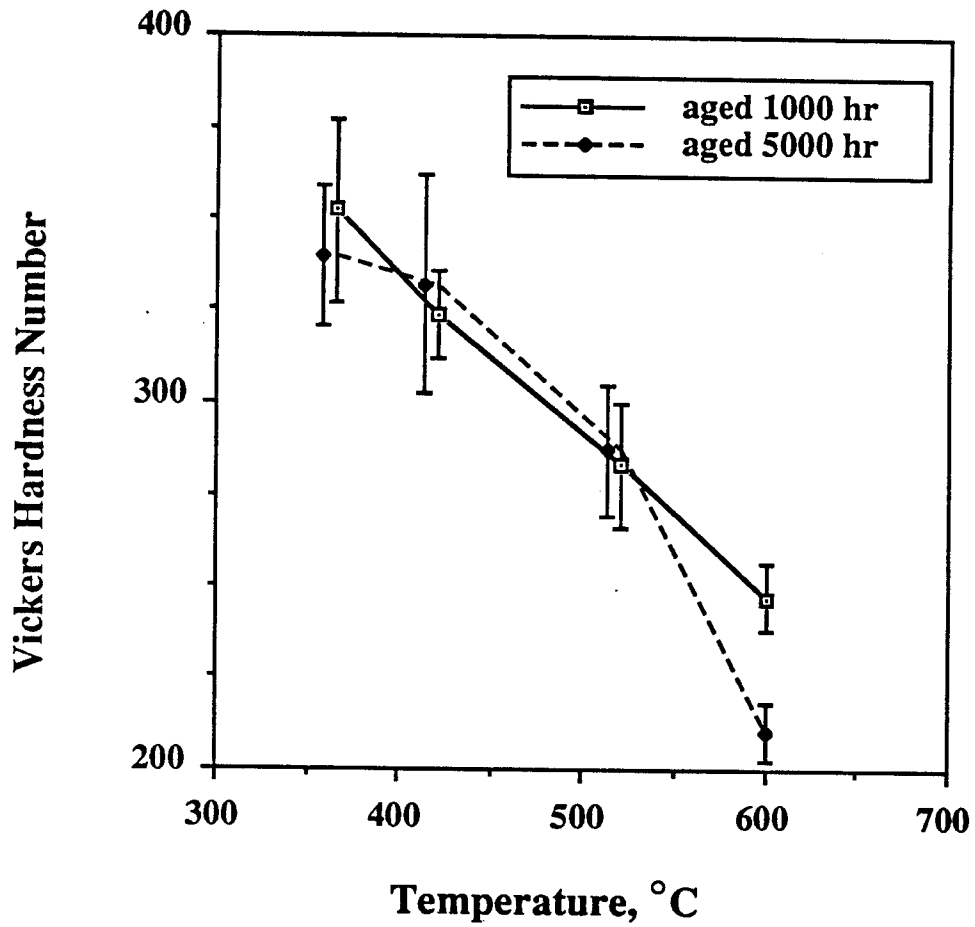


Figure 10. Microhardness results from L9 aged for 1000 and 5000 hours.

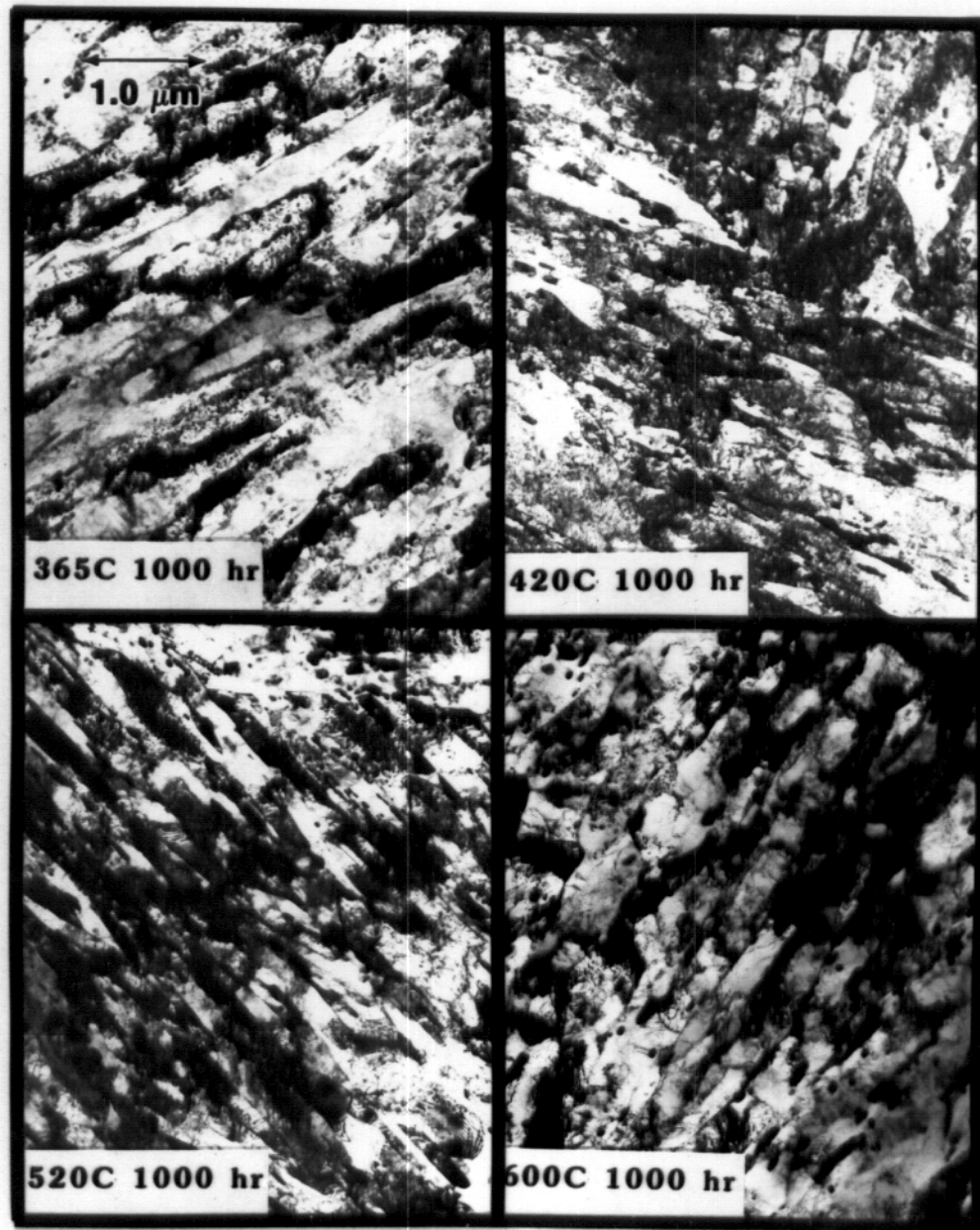


Figure 11. TEM images from L9 aged for 1000 hours.

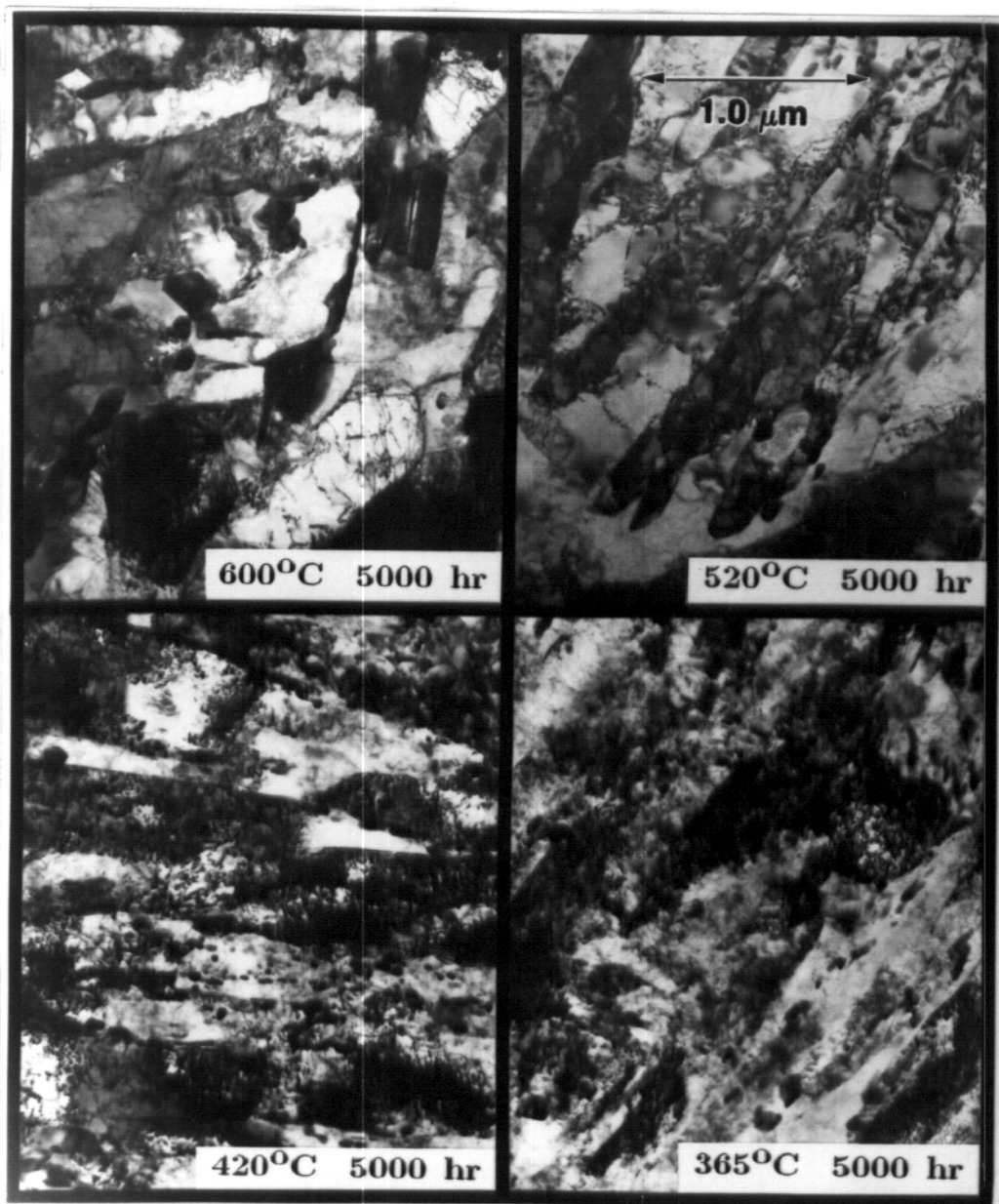


Figure 12. TEM images of L9 aged for 5000 hours.



Figure 13. Equiaxed ferrite grain which is probably a recrystallized ferrite nucleus in L9 aged at 520°C for 5000 hours.

In the steels aged for 1000 hours,  $M_{23}C_6$  was the only precipitate which was found except in the case of the sample aged at 520°C. In this sample, two isolated examples of chi phase were seen. Figure 14a shows a TEM image of the phase. Figure 14b shows the EDS spectrum and 14c is the selected area tilt sequence from chi in a ferrite matrix. The diffraction patterns show a cube-on-cube orientation relationship between chi and the ferrite. In the specimens aged at 420°C for 5000 hours, no chi was found in the extracted precipitates, but in the specimen itself, chi was present in limited amounts. In the specimens aged for 5000 hours at 520°C steel, chi phase was seen in both the steel and in the extracted precipitates. The amount of the chi phase in the precipitates tested was about 15% of the total. The chi phase which was seen in the aged samples was not associated with prior austenite grain boundaries. Chi phase was not found in the samples aged at 600 or 365°C for either 1000 or 5000 hours.

## DISCUSSION

The tempering study indicated that the  $Ac_1$  temperature for the steel lies in the temperature range between 700 and 800°C. The observed hardness increase in the specimens tempered at temperatures above 700°C results from the austenite transforming to new untempered martensite. There was no indication that the tempered samples had formed new austenite at 700°C. The microstructure was that of a well annealed martensitic steel.

Samples which were aged at 365 and 420°C for 1000 and 5000 hours maintained a hardness close to that of the samples tempered at 700°C. However, as the aging temperature increased, the hardness decreased continuously in consequence of the recovery of the dislocation structure and the coarsening of

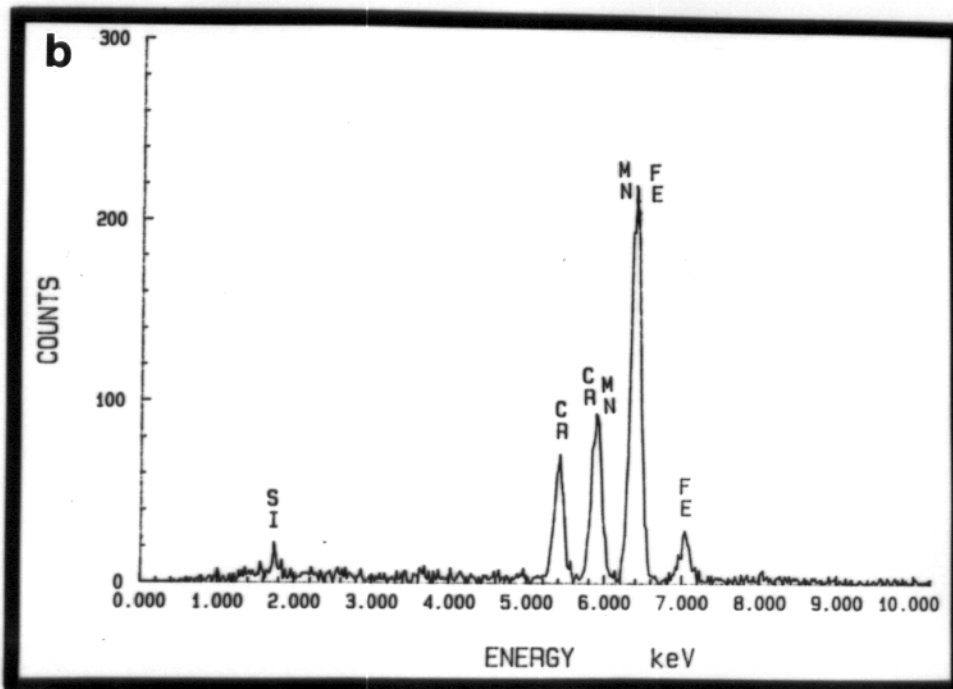
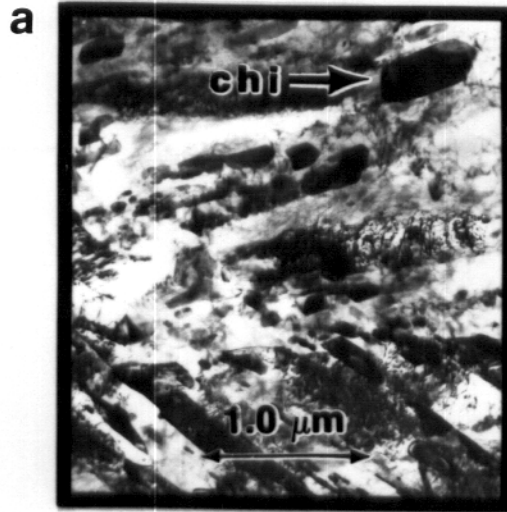


Figure 14. TEM results for chi phase. a) An image of chi embedded in a ferrite matrix. b) EDS spectrum from chi.

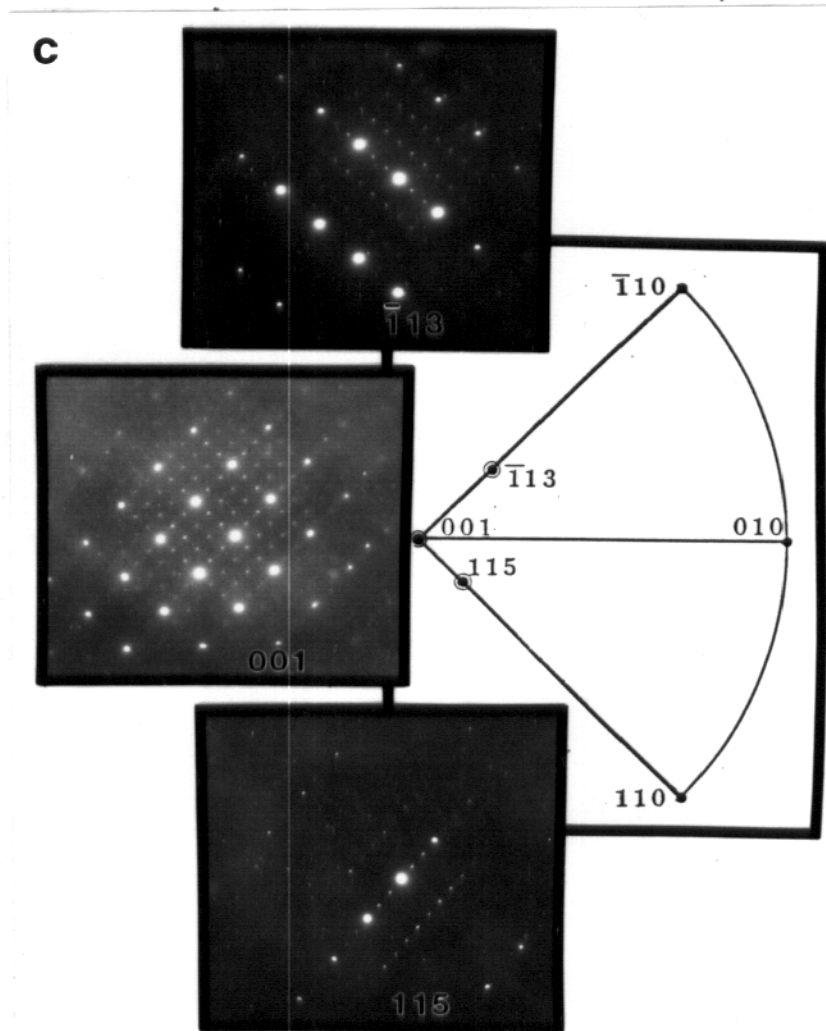


Figure 14. c) SAD tilt sequence from chi showing the cube-on-cube orientation relationship between chi and ferrite.

the precipitates. Also contributing to this hardness decrease was small amounts of recrystallization of the steel aged at temperatures above 420°C.

$M_{23}C_6$  was the major precipitate which formed in the steel during the heat treatments. Tempering at temperatures of 400 and 500°C led to formation of precipitates within the martensite laths which were tentatively identified as  $M_3C$ ; this phase is probably metastable because tempering at 500°C for twenty-four hours caused a mixture of  $M_3C$  and  $M_{23}C_6$  to develop, and at temperatures above 500°C only  $M_{23}C_6$  formed. At all tempering temperatures,  $M_{23}C_6$  was the precipitate which formed at the prior austenite grain boundaries. The chi phase was found in the steel when aged at 520°C for 1000 hours and at 420 and 520°C for 5000 hours. This phase was shown to cause embrittlement when it formed at prior austenite grain boundaries in similar manganese stabilized steels that were irradiated at 365°C to 5.4 dpa.<sup>(6)</sup>

This study has also shown that chi phase can form in high manganese steels in the absence of irradiation although its formation was sluggish and it was only seen at 420 and 520°C.

#### CONCLUSIONS

Tempering and aging of L9 has shown results similar to other 12% Cr martensitic steels.<sup>(7)</sup> The precipitate and matrix structure which developed was not unexpected. The exception was the formation of a manganese-rich chi phase in the samples aged at 420 and 520°C. This phase may be detrimental to the mechanical properties of the steel.

## ACKNOWLEDGEMENT

The authors would like to thank Dr. Brian Vallet and the NORCUS program for supporting this research. We would also like to acknowledge the help of Richard J. Casper with the microscopy.

By acceptance of this article, the publisher and/or recipient acknowledges the U.S. Government's right to retain a nonexclusive, royalty-free license in and to any copyright covering this paper.

This research was supported by the Northwest College and University Association for Science (University of Washington) under Contract DE-AM06-76-RL02225 with the U.S. Department of Energy.

## REFERENCES

1. H.R. Brager, F.A. Garner, D.S. Gelles, and M.L. Hamilton: Journal of Nuclear Materials, 1985, vols. 133 & 134, pp. 907-911.
2. R.L. Klueh, D.S. Gelles, and T.A. Lechtenberg: Journal of Nuclear Materials, 1986, vol. 141-143, pp. 1081-1087.
3. D.S. Gelles and M.L. Hamilton: Journal of Nuclear Materials, 1987, vol. 148, pp. 272-278.
4. D.S. Gelles and M.L. Hamilton, in Alloy Development for Irradiation Performance Semiannual Progress Report for the Period Ending March 31, 1986, DOE/ER-0045/16, pp. 131-139.
5. N.S. Cannon, W.L. Hu and D.S. Gelles, in Fusion Reactor Materials Semiannual Progress Report for the Period Ending March 31, 1987, DOE/ER-0313/2, pp. 119-130.
6. D.S. Gelles and W.L. Hu, in Fusion Reactor Materials Semiannual Progress Report for the Period Ending March 31, 1987, DOE/ER-0313/2, pp. 251-261.
7. E.A. Little, D.R. Harris, F.B. Pickering, and S.R. Keown: Metals Technology, April 1977, pp. 205-217.